# Antenna-Beam Spatial Transformation in C-RAN with Large Antenna Arrays

Zhiyuan Jiang, Sheng Zhou, Zhisheng Niu, *Fellow, IEEE*

***Abstract*—A spatial transformation scheme is proposed to be deployed at the radio-units (RUs) in cloud radio-access-networks (C-RAN) to alleviate the fronthaul burden and baseband signal processing complexity. The module transforms antenna domain signals to the beam domain, such that the spatial dimensionality is significantly reduced for RUs with large antenna arrays. A low-complexity transformation scheme is investigated with finite uplink receive samples. It leverages a combined discrete-Fourier-transform (C-DFT) approach, which shows significant signal power gain over the conventional DFT scheme by combining correlated DFT beams to form a more matched beam pattern. The optimality of the combination method is proved. The performance is validated by extensive simulations which are based on practical channel models and system parameters.**

## I. Introduction

In massive multiple-input multiple-output (MIMO) wireless communication systems, the spectral and radiated energy efficiency can be both boosted by the deployment of massive number of antennas. Moreover, the high beamforming gain of a massive antenna array is the main savior for millimeter wave systems to counteract the high pathloss brought by high frequencies. Therefore, it is extremely important to design high-performance, efficient and practical transmission strategy in massive MIMO systems for the emerging 5G cellular system.

In the implementation of radio access networks (RAN), it is proposed in [1] that a baseband-up centralization architecture, i.e., cloud RAN (C-RAN), can be very helpful in terms of reducing deployment cost, better cooperation and joint signal processing, and more flexible information exchange and processing thanks to the centralized architecture and cloud computing technology [2]. In C-RAN, radio-units (RUs) are distributed in the coverage area and are designed to be as simplified as possible to save both capital (CAPEX) and operational expenditure (OPEX), i.e., "dumb RUs". Take the uplink (UL) signal processing for example, the RUs may be only responsible for the radio frequency (RF) chain processing and signal digitalization. After the processing at RU, the signals are transported to the baseband-unit (BU) via fiber interface, e.g., Common Public Radio Interface (CPRI) [3] or the recently proposed Next Generation Fronthaul Interface (NGFI) [4] by China Mobile. The BU then conducts all baseband processing functionalities for connected RUs. The functionality split between RU and BU is not fixed. Some recent works propose to put more functionalities in the RU so as to save the CPRI capacity [5] [6], e.g., the functionality of physical channels extraction such as the Physical Uplink Shared Channel (PUSCH) in long-term-evolution (LTE) systems.

Despite the merits of both the massive MIMO and C-RAN systems, the marriage of these two poses serious challenges. In practice, it is desirable to deploy a large number of antennas at RU and utilize the split architecture of C-RAN simultaneously [7]–[9]. However, due to the limited capacity of the fronthaul links, it is very unlikely that all antenna ports in the RU can be digitally controlled by the BU. To put it into perspective, based on the current LTE numerology, a bandwidth of 20 MHz of signal which corresponds to a 30.72 MHz sampling rate with each sample being quantized by 30 bits, and a 128-port antenna array requires approximately 157 Gbps fronthaul interface. This quantity exceeds the current CPRI interface (usually around 20 Gbps depending on the number of optical fibers used) by a large margin. Besides, this calculation does not consider the fact that much larger bandwidth will be used in 5G systems, and hence higher interface capacity required. Even for the CPRI upgrade, namely the NGFI, it is clearly required that the fronthaul interface should be independent of the number of antenna ports [4] to avoid such problems.

Fortunately, looking at the channel vector of an antenna array ($M$ is always used to denote the number of the antenna ports at the base station (BS) side), generally it does not span the whole $M$-dimensional linear space due to limited angular spread [10], [11]. The dimensionality deficiency gives us an opportunity to apply the spatial transformation such that the transmission energy is focused in the occurring subspace of the signal and hence the dimensionality is significantly reduced. The most appealing part of leveraging spatial transformation in massive MIMO systems is that with greatly reduced complexity and signaling amount, we can achieve near full-dimension, or possibly better[1] performance.

In practice, it is desirable to have low-complexity spatial transformation schemes, especially when applying to RUs in C-RAN. In literatures, the discrete-Fourier-transform (DFT) based schemes have been extensively studied for the uniform-linear-array (ULA) and uniform-planar-array (UPA). Thanks to the fast-Fourier-transform (FFT) implementations, the DFT-based schemes are very computation-efficient. In addition, it is proved that the DFT approach is asymptotically optimal

This work is sponsored in part by the Nature Science Foundation of China (No. 61571265, No. 61461136004, No. 91638204), and Hitachi R&D Headquarter.

Z. Jiang, S. Zhou and Z. Niu are with Tsinghua National Laboratory for Information Science and Technology, Tsinghua University, Beijing 100084, China. Emails: zhiyuan@tsinghua.edu.cn; sheng.zhou@tsinghua.edu.cn; niuzhs@tsinghua.edu.cn.

[1]This relates to channel estimation issues with per-antenna processing [12].

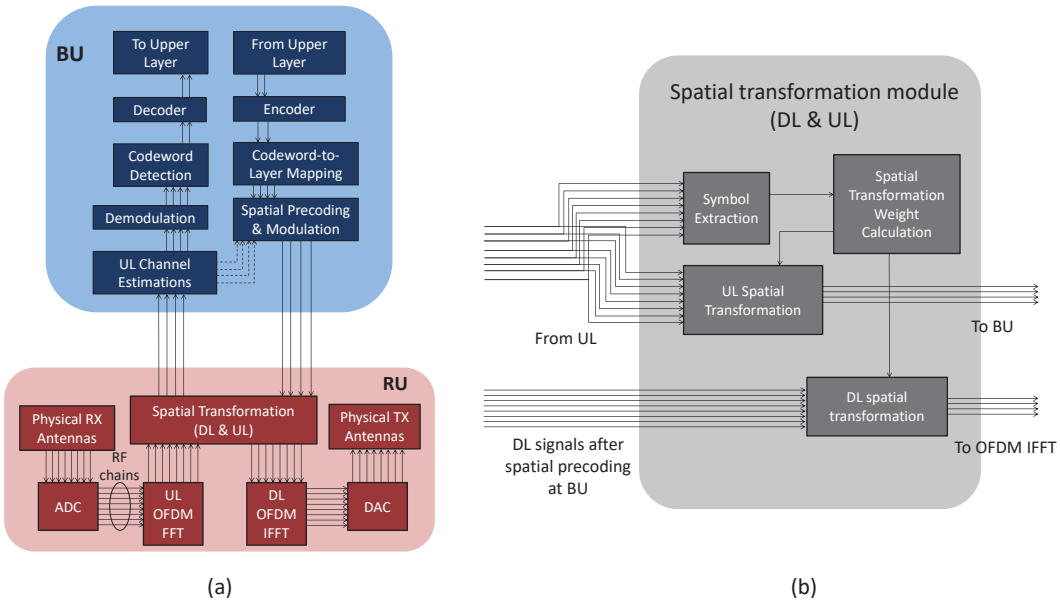


Fig. 1. Proposed schematic and signal flow of the C-RAN architecture including spatial transformation.

in the large array regime [10], on the condition of *infinite* channel output samples such that the channel is ergodic in the sense that time average of the channel correlation matrix (CCM) converges to the ensemble average. However, such a condition seldom presents itself with realistic system numerologies due to two reasons. Firstly, the CCM estimation period cannot be infinite considering delay constraints and processing complexity. Secondly, with realistic user mobility and propagation environments, more often than not the channel is not ergodic in the estimation period. Take an LTE typical numerology for example, a user with 3 km/h moving speed in a system with 3 GHz carrier frequency moves approximately $0.01$ wavelengths in one subframe (1 ms). Hence, the channel is most likely to stay relatively static, rather than experience all the channel states as required by the ergodicity condition, in the subframe.

In this paper, we propose to adopt a novel spatial transformation scheme at RU side. The system architecture is presented in Fig. 1. A combined DFT beams approach is proposed which leverages the fact that with finite samples, most DFT beams are not sufficiently decorrelated. Therefore, it is beneficial to combine DFT beams with strong correlations to further reduce the signal dimensionality. The proposed scheme, referred to as the combined DFT scheme (C-DFT), is still computationally efficient, with slightly additional complexity compared with the DFT scheme. Simulation results with realistic LTE system numerologies are presented which compare the performance of C-DFT and DFT schemes with various channel parameters.

## II. Problem Formulations and Preliminaries

Consider a single-cell model, where the uplink receive signal of a BS with $M$ co-located antenna elements, assuming orthogonal-frequency-division-multiplexing (OFDM) systems, can be written as

$$\boldsymbol{y}_{l,t} = \boldsymbol{H}_{l,t}\boldsymbol{x}_{l,t} + \boldsymbol{n}_{l,t}, \tag{1}$$

where $l \in \{1, ..., L\}$ denotes the subcarrier index, $t \in \{1, ..., T\}$ denotes the time index, the total number of subcarriers and time slots are denoted by $L$ and $T$, respectively. $\boldsymbol{H}_{l,t}$ is the corresponding uplink channel transfer matrix with dimension $M \times U$, $\boldsymbol{x}_{l,t}$ denotes the $U$-dimensional uplink data streams which can be from different users or different spatial layers of a single user, and $\boldsymbol{n}_{l,t}$ denotes the Gaussian white addictive noise.

The problem is that given the finite set of channel output samples, i.e., $\boldsymbol{y}_{l\in\{1,...,L\},t\in\{1,...,T\}}$, design a spatial transformation matrix $\boldsymbol{F}$ with dimensions $M \times B$ ($B \leq M$) where $B$ is the number of beams, such that the spatial dimensionality of the receive signal is reduced as

$$\bar{\boldsymbol{y}}_{l,t} = \boldsymbol{F}^{\dagger}\boldsymbol{y}_{l,t}, \tag{2}$$

where $(\cdot)^{\dagger}$ denotes the conjugate transpose. The transformed signal $\bar{\boldsymbol{y}}_{l,t}$ is then used for subsequent signal processing, e.g., channel estimations and demodulations. The metric adopted for evaluating spatial transformation schemes is the transform efficiency which is defined as the signal power ratio between the signal after the transform and before that, i.e.,

$$\eta(\boldsymbol{F}) = \frac{\sum_{l,t} \|\bar{\boldsymbol{y}}_{l,t}\|_{\mathrm{F}}}{\sum_{l,t} \|\boldsymbol{y}_{l,t}\|_{\mathrm{F}}} = \frac{\sum_{l,t} \left\|\boldsymbol{F}^{\dagger}\boldsymbol{y}_{l,t}\right\|_{\mathrm{F}}}{\sum_{l,t} \|\boldsymbol{y}_{l,t}\|_{\mathrm{F}}}, \tag{3}$$

where $\|\cdot\|_{\mathrm{F}}$ denotes the Frobenius norm. Note that here it is prescribed that $\boldsymbol{F}$ has orthonormal columns such that the transform efficiency is well defined with range $\eta(\boldsymbol{F}) \in [0, 1]$.

### A. Ensemble-Average and Time-Average CCM

The ensemble-average of the CCM is defined as

$$\boldsymbol{R} = \mathbb{E}\left[\boldsymbol{H}\boldsymbol{H}^{\dagger}\right], \tag{4}$$

where $\boldsymbol{H}$ is the uplink channel matrix and the frequency and time indexes are omitted assuming the channel statistics is static in the period. Note that most existing work adopts the ensemble-average in the system and algorithm design, whereas in practice only the time-average of the CCM is available. One widely-used CCM estimation without any dedicated pilots is

$$\bar{\boldsymbol{R}} = \frac{1}{TL} \sum_{t=1,...,T;\, l=1...,L} \boldsymbol{y}_{t,l} \boldsymbol{y}_{t,l}^{\dagger} - \boldsymbol{\Lambda}, \tag{5}$$

where $\boldsymbol{\Lambda}$ is the interference and noise covariance matrix. In the case of Gaussian white noise with variance $\sigma^2$, $\boldsymbol{\Lambda} = \sigma^2 \boldsymbol{I}$. The interference covariance can be either obtained by the subsequent processing blocks, or ignored with no prior channel knowledge required.

### B. DFT Scheme

From a broader perspective, the DFT scheme is an inner-product based angle-of-arrival (AoA) estimation algorithm. Essentially, it leverages the limited angular spread of receive signals in cellular systems, in the sense that if the total angular domain is divided into several angular bins, the number of bins that effectively contain all signal power is usually smaller than the number of BS antennas. Therefore, it is beneficial to transmit in the dominant angular bins which constitute the subspace we mentioned earlier. The scheme can be implemented on ULAs and UPAs very computation-efficiently based on the FFT algorithms. Specifically, first $\tau$ hypothesis beams, each representing a angular bin, are generated as $\boldsymbol{D} = [\boldsymbol{d}_1, ..., \boldsymbol{d}_\tau]$. Denote the testing matrix as

$$\boldsymbol{\Gamma} = \boldsymbol{D}^{\dagger} \boldsymbol{R} \boldsymbol{D}. \tag{6}$$

Then the diagonal elements of $\boldsymbol{\Gamma}$ represent the power estimated at the AoA of corresponding $A$ DFT beams. Due to the structure of the DFT beams, the testing matrix can be efficiently calculated if the $A$ hypothesis beams are selected such that their AoAs are uniformly distributed in the directional cosine domain. Based on $\boldsymbol{\Gamma}$, the spatial transformation matrix is selected such that it contains the $B$ strongest beams.

## III. Algorithm Description

In this section, we first use a simple example to illustrate why the DFT scheme is not optimal in the finite-sample case, which factors affect the finite-sample performance, and how to improve it. Then the C-DFT scheme is proposed and the optimality proof is given in terms of transform efficiency with finite samples.

### A. Single Scattering Cluster Example

Consider a simplified channel model, where there is one single-antenna user and one scattering cluster, as shown in Fig. 2. Assume the incoming AoAs are uniformly distributed in the angular spread $(\theta, \psi)$, i.e, denote the AoA set as

$$\mathcal{A} = \left\{ (\gamma, \phi) : \gamma \in \mathrm{U}\left[-\frac{\theta}{2}, \frac{\theta}{2}\right], \phi \in \mathrm{U}\left[-\frac{\psi}{2}, \frac{\psi}{2}\right] \right\}, \tag{7}$$

where $\gamma$ and $\phi$ denote the azimuth and elevation AoAs respectively, and $\mathrm{U}[\cdot]$ denotes the uniform distribution. The

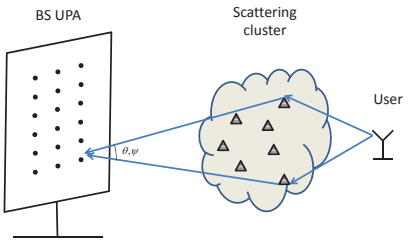


Fig. 2. Propagation environments with a single scattering cluster.

uplink channel vector is then the superposition of all relevant paths

$$\boldsymbol{h}_{l,t} = \frac{1}{\theta\psi} \int_{(\gamma,\phi)\in\mathcal{A}} \beta_{l,t}(\gamma,\phi) \boldsymbol{d}(\gamma,\phi)\, \mathrm{d}\gamma \mathrm{d}\phi, \tag{8}$$

where $\beta_{l,t}(\gamma,\phi)$ is the amplitude of the corresponding beam at instance $(l,i)$ which is affected by small-scale fading, and $\boldsymbol{d}(\gamma,\phi)$ is a DFT vector (or Kronecker product of two DFT vectors) when ULA or UPA is considered.

Given the scattering environment, let us consider the number of beams that are needed to capture all the signal power based on the DFT scheme, and the minimum number of beams given finite samples. The following claims are proposed.

- In the large antenna array regime, the DFT scheme needs approximately $M\rho$ beams, where $\rho$ is the span of $\mathcal{A}$ in the directional cosine domain [13].
- The minimum number of beams needed when finite samples are given depends on the channel ergodicity. In the extreme case of static channel during the sampling period, only one beam is sufficient.

The first claim is based on the fact that the signal power is uniformly distributed in $\mathcal{A}$, and therefore all the DFT beams with $(\gamma,\phi) \in \mathcal{A}$ carry signal power. The number of such beams is $M\rho$ as proved by [13]. The channel ergodicity in the second claim relates to how much the small-scale fading is averaged during the sampling period, more specifically, the ergodicity of random variable $\beta_{l,t}(\gamma,\phi)$. In the extreme case of that the scattering environment and the user is static during the sampling period, i.e.,

$$\boldsymbol{h}_{l,t} = \boldsymbol{h}_{\mathrm{c}};\, (l = 1, ..., L,\, t = 1, ..., T), \tag{9}$$

only one beam $\frac{\boldsymbol{h}_{\mathrm{c}}}{\|\boldsymbol{h}_{\mathrm{c}}\|_F}$ is needed to capture all the signal power. Therefore, it is clear that with finite samples when limited channel ergodicity comes into play, there is significant room to improve the DFT scheme. Specifically, the channel ergodicity relies on several factors, such as user mobility, scattering environment changing speed, the length of the sampling period, and the carrier frequency. No matter which factors are relevant, it is found that correlations exist among the selected DFT beams, which motivate the proposed C-DFT scheme described in the following subsection.

### B. Proposed C-DFT Scheme

In a nutshell, the C-DFT scheme first selects a number of DFT beams (more than the required number eventually) based on the DFT scheme, and then checks the correlation matrix

of the beams during the sampling period to further combine them into the final beams. The detailed procedure is described for UPA in Algorithm 1.

**Algorithm 1** C-DFT

**Input:** A block (time and frequency) of uplink receive signals after OFDM FFT, $\boldsymbol{y}_{l,t}$; The number of DFT beams that are selected after the DFT scheme, $B_{\rm d}$; The number of final beams that are selected, $B$;

**Output:** The spatial transformation matrix $\boldsymbol{F}\,(M \times B)$;

1: Calculate the time-averaged CCM $\bar{\boldsymbol{R}}$ based on (5).
2: Select $M$ DFT beams with equal angular spacing in the angular cosine domain, i.e., $\boldsymbol{D} = [\boldsymbol{d}_1, ..., \boldsymbol{d}_M]$;
3: Calculate $\boldsymbol{\Gamma} = \boldsymbol{D}^\dagger \bar{\boldsymbol{R}} \boldsymbol{D}$, and select $B_{\rm d}$ columns in $\boldsymbol{D}$ which correspond to the $B_{\rm d}$ largest diagonal elements of $\boldsymbol{\Gamma}$, i.e., without loss of generality, $\boldsymbol{F}_{\rm D} = [\boldsymbol{d}_1, ..., \boldsymbol{d}_{B_{\rm d}}]$;
4: Denote the uplink signals after the DFT scheme as $\boldsymbol{y}_{{\rm d},l,t} = \boldsymbol{F}_{\rm D}^\dagger \boldsymbol{y}_{l,t}$, and calculate $\bar{\boldsymbol{R}}_{\rm d} = \frac{1}{TL}\sum_{t,\,l} \boldsymbol{y}_{{\rm d},l,t} \boldsymbol{y}_{{\rm d},l,t}^\dagger$;
5: Do the singular-value-decomposition (SVD) of $\bar{\boldsymbol{R}}_{\rm d}$, i.e., $\bar{\boldsymbol{R}}_{\rm d} = \boldsymbol{U}\boldsymbol{S}\boldsymbol{U}^\dagger$, and select the first $B$ columns of $\boldsymbol{U}$ to form $\boldsymbol{F}_{\rm S}$;
6: **return** $\boldsymbol{F} = \boldsymbol{F}_{\rm D}\boldsymbol{F}_{\rm S}$.

In order to check the correlations among the $B_{\rm d}$ DFT beams, the SVD method[2] is selected as in Step 5. The performance is guaranteed by the following theorem.

*Theorem 1:* Given finite samples of receive signal vectors of dimension $N$, i.e., $\boldsymbol{r}_{l,t}$ $(l = 1, ..., L;\, t = 1, ..., T)$, and the first $N_{\rm s}$ $(N_{\rm s} \le N)$ columns of the singular matrix of $\bar{\boldsymbol{R}} = \frac{1}{TL}\sum_{t,\,l} \boldsymbol{r}_{l,t}\boldsymbol{r}_{l,t}^\dagger$ as $\boldsymbol{F}_{\rm U}$, and the set $\mathcal{F} = \left\{\boldsymbol{F} :\, \boldsymbol{F} = \boldsymbol{F}_{\rm U}\boldsymbol{V},\, \boldsymbol{V}\boldsymbol{V}^\dagger = \boldsymbol{V}^\dagger\boldsymbol{V} = \boldsymbol{I}_{N_{\rm s}}\right\}$, then for any $\boldsymbol{F}_{\rm opt} \in \mathcal{F}$,

$$\boldsymbol{F}_{\rm opt} = \underset{\boldsymbol{F}\in\mathbb{H}_{N_{\rm s}}}{\arg\max}\ \eta(\boldsymbol{F}), \tag{10}$$

and,

$$\eta(\boldsymbol{F}_{\rm opt}) = \frac{\sum_i^{N_{\rm s}} \lambda_i}{\sum_i^{N} \lambda_i}, \tag{11}$$

where $\mathbb{H}_{N_{\rm s}}$ denotes the space of all $N \times N_{\rm s}$ matrices $\boldsymbol{F}$ with orthonormal columns, $\lambda_i$ $(i = 1, ..., N)$ are the singular values of $\bar{\boldsymbol{R}}$, and $\eta(\boldsymbol{F})$ is defined in (3).

*Proof:* Consider the transform efficiency maximization problem,

$$\begin{aligned} \max_{\boldsymbol{F}} \quad & \eta(\boldsymbol{F}) \\ \text{s.t.} \quad & \boldsymbol{F} \in \mathbb{H}_{N_{\rm s}}, \end{aligned} \tag{12}$$

wherein the objective can be derived as

$$\eta(\boldsymbol{F}) = \frac{\sum_{l,t} \left\|\boldsymbol{F}^\dagger \boldsymbol{y}_{l,t}\right\|_{\rm F}}{\sum_{l,t} \left\|\boldsymbol{y}_{l,t}\right\|_{\rm F}} = \frac{{\rm tr}\left[\boldsymbol{F}^\dagger \bar{\boldsymbol{R}} \boldsymbol{F}\right]}{{\rm tr}\,\bar{\boldsymbol{R}}}, \tag{13}$$

where tr$[\cdot]$ denotes the trace of a matrix. Denote the SVD as $\bar{\boldsymbol{R}} = \boldsymbol{U}\boldsymbol{S}\boldsymbol{U}^\dagger$, and $\boldsymbol{G} = \boldsymbol{U}^\dagger\boldsymbol{F}$ which is a bijection in $\mathbb{H}_{N_{\rm s}} \to \mathbb{H}_{N_{\rm s}}$. Therefore, it is equivalent to substitute $\bar{\boldsymbol{R}}$ in (13) for $\boldsymbol{S}$.

[2]We always assume the singular values are arranged in descending order in the SVD method.

Denote $\boldsymbol{G} = \left[\boldsymbol{G}_{N_{\rm s}}^\dagger,\, \boldsymbol{G}_{N-N_{\rm s}}^\dagger\right]^\dagger$, where $\boldsymbol{G}_{N_{\rm s}}$ is a square matrix and $\boldsymbol{G}_{N-N_{\rm s}}$ is what remains. It follows that

$$\begin{aligned} \eta(\boldsymbol{F}) &= \frac{{\rm tr}\left[\boldsymbol{G}^\dagger \boldsymbol{S} \boldsymbol{G}\right]}{{\rm tr}\,\boldsymbol{S}} \\ &= \frac{{\rm tr}\left[\boldsymbol{G}_{N_{\rm s}}^\dagger \boldsymbol{S}_1 \boldsymbol{G}_{N_{\rm s}}\right] + {\rm tr}\left[\boldsymbol{G}_{N-N_{\rm s}}^\dagger \boldsymbol{S}_2 \boldsymbol{G}_{N-N_{\rm s}}\right]}{{\rm tr}\,\boldsymbol{S}} \\ &\le \frac{{\rm tr}\,\boldsymbol{S}_1 {\rm tr}\left[\boldsymbol{G}_{N_{\rm s}} \boldsymbol{G}_{N_{\rm s}}^\dagger\right] + \lambda_{N_{\rm s}+1} {\rm tr}\left[\boldsymbol{G}_{N-N_{\rm s}} \boldsymbol{G}_{N-N_{\rm s}}^\dagger\right]}{{\rm tr}\,\boldsymbol{S}} \\ &\le \frac{{\rm tr}\,\boldsymbol{S}_1}{{\rm tr}\,\boldsymbol{S}}, \end{aligned} \tag{14}$$

where $\boldsymbol{S}_1$ and $\boldsymbol{S}_2$ are diagonal matrices containing the first $N_{\rm s}$ and the last $N - N_{\rm s}$ diagonal elements. It is straightforward to observe that the equality holds if $\boldsymbol{G}_{N_{\rm s}}$ is a orthonormal matrix, such that the solution to (12) is the first $N_{\rm s}$ $(N_{\rm s} \le N)$ columns of the singular matrix of $\bar{\boldsymbol{R}}$ multiplied by an arbitrary $N_{\rm s}$-dimensional orthonormal matrix. ■

Theorem 1 shows that the optimal spatial transformation matrix in $\mathbb{H}_{N_{\rm s}}$ with finite samples can be obtained by performing the SVD on the time-averaged CCM. Therefore, the SVD on the beam space signal in Algorithm 1 is the optimal way to combine the DFT beams. Alternatively, one can perform the SVD on the original received signal, i.e., $\boldsymbol{y}_{l,t}$, which is referred to as the SVD scheme. However, the complexity of the SVD on an $M$-dimensional matrix may be too high in some scenario, e.g., spatial transformation implemented on the RU. In comparison, the C-DFT scheme only needs to perform SVD on a $B_{\rm d}$-dimensional matrix. A complexity analysis is given below.

### C. Complexity Analysis

In the analysis, the computational complexity of the main signal processing steps, including the DFT ($\mathcal{O}(n\log(n))$) and SVD ($\mathcal{O}(n^3)$) operations are compared among the DFT, SVD and C-DFT schemes. The complexity of calculating the CCM is ignored since it is the same for all schemes (The CCM calculation of $\bar{\boldsymbol{R}}_{\rm d}$ in Step 4 in C-DFT can be obtained from $\Gamma$). In the DFT and C-DFT schemes, the beam testing step, i.e., the calculation of $\Gamma$ can be efficiently implemented by the FFT algorithm for ULAs and UPAs. The detailed implementation is omitted for brevity. The analysis is shown in Table I. It will be shown in the simulation results that $B_{\rm d}$ is usually much smaller than $M$. Therefore the C-DFT scheme only introduces slightly larger computational complexity compared to the DFT scheme.

TABLE I
COMPLEXITY ANALYSIS

| | DFT | C-DFT | SVD |
|---|---|---|---|
| Complexity (flops) | $\mathcal{O}\big(M^2\log(M)\big)$ | $\mathcal{O}\big(M^2\log(M) + B_{\rm d}^3\big)$ | $\mathcal{O}(M^3)$ |

## IV. SIMULATION RESULTS

In this section, the simulation results are presented which are based on a 3rd-Generation-Partnership-Project (3GPP)

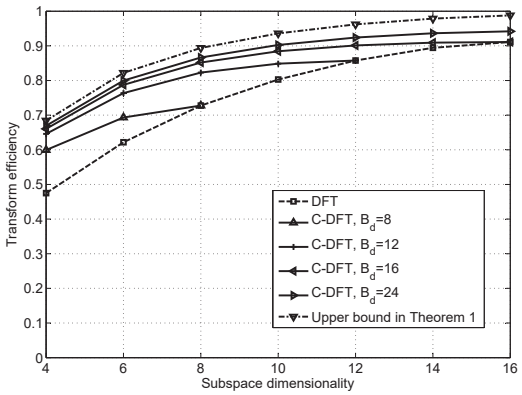


Fig. 3. Transform efficiency comparisons between C-DFT and DFT. The user moving speed is 3 km/h, and the sampling period is 1 ms.

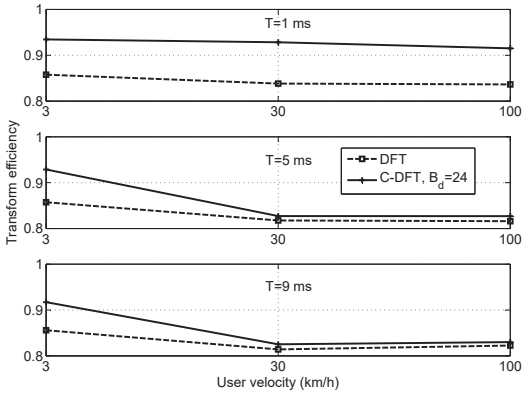


Fig. 4. The impact of channel ergodicity and sampling length. The subspace dimensionality is 10.

spatial channel model (SCM) and LTE numerologies. The spatial transformation module is inserted in the uplink processing chain, between the OFDM FFT and the channel estimation modules. The carrier frequency is 2.6 GHz with an uplink signal bandwidth of 20 MHz. The OFDM configuration is based on 15 KHz subcarrier spacing and 2048-point FFT. The BS antenna array is a UPA with 128 ports (16 columns $\times$ 4 rows $\times$ 2 polarizations), $0.5\lambda$ antenna spacing in both horizontal and vertical domains[3]. The SCM adopted is the urban-macro scenario, where a total of 6 rays for each user (a total of 4 users uniformly spread in the angular domain) are considered. The amplitude of each ray is Rican distributed representing small-scale fading determined by user location and mobility. A detailed description of the SCM can be found in [14]. The uplink receive signal-to-noise-ratio (SNR) per antenna port is set to 0 dB. The time/frequency granularity is one LTE subframe (14 OFDM symbols for 1 ms duration and 1200 subcarriers), i.e., the minimum sampling period is one subframe. The simulation runs for 400 subframes.

It is observed from Fig. 3 that the beam combination in the C-DFT scheme gives it significant advantage over the DFT scheme in terms of transform efficiency with limited subspace dimensionality (number of selected beams). The upper bound in the figure is calculated based on Theorem 1 with full-dimensional signals. Moreover, the number of DFT beams needed in the C-DFT scheme is quite small, in which case 16 beams (with 128 ports) are sufficient to achieve near-optimal performance. Thereby the additional complexity introduced by SVD operation in the C-DFT scheme is relatively low. The C-DFT and the DFT schemes have identical performance when the number of DFT beams equals the subspace dimensionality, due to the fact that the beam combining of the C-DFT scheme in this case is merely a beam rotation without dimensionality reduction.

Fig. 4 shows the impact of finite samples on the spatial transformation schemes. Particularly, we change the user moving speed and the time period for CCM averaging to have different channel ergodicity and sampling length, respectively. It is observed that generally, more ergodic channel and longer sampling period result in that the time-average CCM converges more to the ensemble-average CCM, and hence narrower performance gap between the C-DFT and DFT schemes, since the advantage of the C-DFT scheme relies on the correlations among DFT beams.

### A. Link-Level Simulations

In order to validate the proposed spatial transform performance in practice and also the transform efficiency metric we adopt for evaluation, a link-level LTE-based simulation is conducted. The spatial transform is performed as described in Fig. 1. After the spatial transformation, the channel estimation scheme adopted is a FFT-based scheme [15], and the baseband receiving algorithm to decode multi-user signals is MMSE-based. After the MMSE receiver, the decoded constellation points for the user are compared with the transmit ones to calculate the symbol-error-rate (SER). The simulator does not include channel coding and decoding to save processing time. The SINR is mapped from the SER based on a predefined look-up table (with different modulation orders) and thereby the throughput is calculated based on the Shannon formula. The simulator only calculates the throughput of the first user for simplicity, and averaged over multiple drops. Therefore, the resulting throughput can be interpreted as per-user throughput. The link adaptation is enabled to support various SNRs. All users are scheduled simultaneously (traffic type: full buffer) on the whole frequency bandwidth. We simulate each drop for 200 ms, which corresponds to 20 radio frames in the LTE systems.

Fig. 5 shows the comparison for a typical scenario, where the BS has 128 antenna ports, i.e., $4 \times 16 \times 2$ (rows $\times$ columns $\times$ polarizations), and the number of beams after spatial transformation is 8. The number of selected DFT beams in the DFT-SVD scheme is varied from 4 to 16. It is observed that the DFT-SVD scheme with selected DFT-beams of 32 is very close to the optimal SVD scheme with greatly reduced complexity.

[3]The extension of the proposed scheme to cross polarizations is straightforward by following the same procedure for each polarization assuming no polarization leakage.

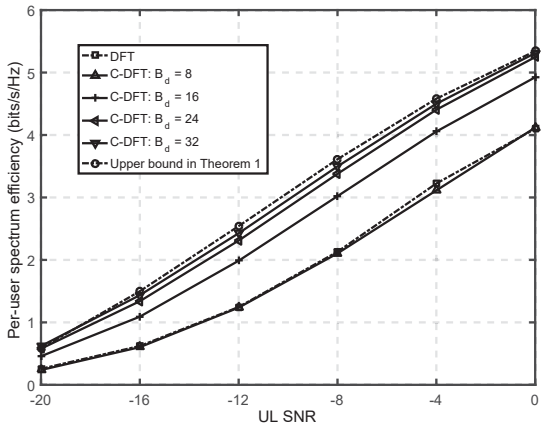


Fig. 5. Comparisons of spatial transformation schemes for different SNRs.

## V. Conclusions

In this paper, we propose the combined DFT scheme to be implemented as the spatial transformation scheme in C-RAN systems, which leverages the correlations among DFT beams during the sampling period to improve the transform efficiency compared with the conventional DFT scheme. It is found that the additional complexity over the DFT scheme is marginal, and that the performance improvements are evident based on link-level simulations with a 3GPP channel model and practical system parameters. The advantage are especially significant with limited uplink receive symbols.

## References

[1] K. Chen and R. Duan, "C-RAN–the road towards green RAN," *China Mobile Research Institute, White Paper*, 2011.

[2] Z. Jiang, S. Zhou, and Z. Niu, "Optimal antenna cluster size in cell-free distributed large-scale antenna systems with imperfect CSI and inter-cluster interference," *IEEE Trans. Veh. Technol.*, vol. PP, no. 99, pp. 1–1, 2014.

[3] "CPRI specification v6.0," 2013.

[4] J. Huang and Y. Yuan, "Next generation fronthaul interface, NGFI," *China Mobile Research Institute, White Paper*, 2015.

[5] J. Liu, S. Zhou, J. Gong, Z. Niu, and S. Xu, "Graph-based framework for flexible baseband function splitting and placement in C-RAN," in *Proc. IEEE International Conference on Communications (ICC)*, pp. 1958–1963, Jun 2015.

[6] J. Liu, S. Xu, S. Zhou, and Z. Niu, "Redesigning fronthaul for next-generation networks: beyond baseband samples and point-to-point links," *IEEE Wireless Commun.*, vol. 22, pp. 90–97, Oct. 2015.

[7] "Cloud RAN introduction. the 4th CJK international workshop technology evolution and spectrum," *Shenzhen, China*, Sep. 2011.

[8] "ZTE green technology innovations white paper," *Shenzhen, China*, 2011.

[9] "Intel heterogenous network solution brief," *Santa Clara, CA, USA*, 2011.

[10] A. Adhikary, J. Nam, J.-Y. Ahn, and G. Caire, "Joint spatial division and multiplexing: The large-scale array regime," *IEEE Trans. Inform. Theory*, vol. 59, pp. 6441–6463, Oct. 2013.

[11] Z. Jiang, A. Molisch, G. Caire, and Z. Niu, "Achievable rates of FDD massive MIMO systems with spatial channel correlation," *IEEE Trans. Wireless Commun.*, vol. 14, pp. 2868–2882, May 2015.

[12] S. Haghighatshoar and G. Caire, "An active-sensing approach to channel vector subspace estimation in mm-wave massive MIMO systems," *arXiv preprint arXiv:1511.01634*, 2015.

[13] Z. Jiang, S. Zhou, and Z. Niu, "On dimensionality loss in FDD massive MIMO systems," in *Proc. IEEE Conference on Wireless Communications and Networking (WCNC)*, Mar. 2015.

[14] D. S. Baum, J. Hansen, and J. Salo, "An interim channel model for beyond-3G systems: extending the 3GPP spatial channel model (SCM)," in *IEEE Vehicular Technology Conference (VTC)*, vol. 5, pp. 3132–3136 Vol. 5, May 2005.

[15] P. Tan and N. C. Beaulieu, "A comparison of DCT-based OFDM and DFT-based OFDM in frequency offset and fading channels," *IEEE Trans. Commun.*, vol. 54, pp. 2113–2125, Nov 2006.